ELSEVIER

Polymer 41 (2000) 8393–8400

polymer

www.elsevier.nl/locate/polymer

Cold crystallization effects in free charge relaxation in PET and PEN

J.C. Cañadas*, J.A. Diego, J. Sellarès, M. Mudarra, J. Belana

Universitat Politècnica de Catalunya, Departament de Física i Enginyeria Nuclear, ETSEIT, C.Colom, 11-08222 Terrassa, Barcelona, Spain

Received 28 October 1999; received in revised form 31 January 2000; accepted 9 March 2000

Abstract

A comparative study of free charge relaxation in amorphous and partially crystallized poly(ethylene-2,6-naphthalene dicarboxylate) (PEN) and poly(ethylene terephthalate) (PET) has been carried out by thermally stimulated depolarization currents (TSDC), differential scanning calorimetry (DSC), and X-ray diffraction. Amorphous films have been crystallized thermally at temperatures between 170 and 200°C (PEN); 100 and 150°C (PET) by the thermal stimulation by steps method. The windowing polarization (WP) technique has been applied to form PET and PEN thermoelectrets. TSDC of these electrets polarized at 86°C (PET) and 130°C (PEN) show only one peak which is attributed to space charge relaxation (ρ peak). The evolution of this peak has been fitted to the general kinetic order model. DSC measurements of these samples show the appearance of a small endothermic prefusion peak once the crystallization of the sample is completed. This peak increases and shifts towards higher temperatures as the sample is further thermally treated. Associated with the appearance of this endothermic peak, the ρ relaxation passes through a maximum with a sharp decrease with further heat temperature. The X-ray diffraction measurements of these samples show that the decrease in the ρ peak is associated with the improvement of the amorphous–crystal interphases.

Keywords: Crystallinity; Thermostimulated depolarization current; Windowing polarization

1. Introduction

Poly(ethylene-2,6-naphtalene dicarboxylate) (PEN) and poly(ethylene terephthalate) (PET) are interesting polymers fulfilling new electrical and mechanical engineering demands. They exhibit superior thermal stability, mechanical and tensile properties than other polyesters. Their properties are suitable for technological applications such as commercial recipients, insulating in surface mounted technology, miniaturization of capacitors or as a base film for long-playing videotapes. These applications require however a wide knowledge of the electrical behavior in a broad spectrum of environmental conditions. In this sense, the combination of thermally stimulated depolarization currents (TSDC) measurements of samples polarized by windowing polarization (WP) with other characterization techniques, such as differential scanning calorimetry (DSC) and X-ray diffraction, represents a powerful experimental tool set to characterize the material in several aspects.

TSDC has been applied in the last few decades to study electrical relaxations in polymers. In this technique, bound and free charges in the material are activated by a polarizing field at high temperature for a poliarization time, and then frozen by cooling the sample to form an electret. In the conventional formation of an electret, the sample is cooled while the filed remains applied on it. It is possible as well to remove the polarizing field just at the beginning of the cooling process or a few degrees below. This procedure is known as WP [1–8] and it is used to resolve the complex TSDC spectrum of conventionally polarized samples into its elementary Debye like components. In the conventional methods the frozen-in charges are related to a wide range of trapping levels or relaxation times [9]. In the case of WP, the charge trapped is associated with a narrow interval of trapping depths, so that it may result in a simpler interpretation of the results. After WP, the sample is depolarized heating at a constant rate while the resulting current intensity is recorded as a function of temperature. At temperatures above T_g, the ρ relaxation appears, which is related to the free charge trapped in the polymer. Discharges of electrets polarized by WP at several polarization temperatures show an optimal polarization temperature T_{po} [9–11] at which the discharge peak exhibits a maximum area.

TSDC curves of electrets formed by WP can be fitted to different models that consider a unique relaxation time. In this work, we have employed the general kinetic order model to analyze the experimental results obtained from the TSDC technique. Within this model, the current

* Corresponding author.

0032-3861/00/$ - see front matter
PII: S0032-3861(00)00192-0

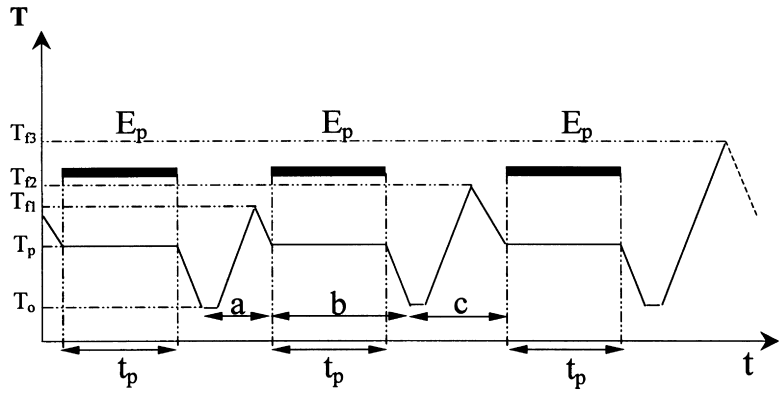

Fig. 1. Schematic representation of the TSS method, (a), (c) TSDC measurements and partial crystallization, (b) polarization.

intensity is given by

$$I = -\frac{dn}{dt} = n^b s_0 \exp\left(-\frac{E_a}{kT}\right) \quad (1)$$

The model is characterized by four parameters: n_0 is the initial trapped charge and it is needed to integrate Eq. (1), s_0 is the preexponential frequency factor, E_a is the activation energy (or trap depth in this model) and b is the kinetic order, an empirically determined parameter.

The b parameter is related to the interplay between the retrapping and the recombination rates. Only kinetic order values $b = 1$ and $b = 2$ have a clear physical meaning. The value $b = 1$ corresponds to the slow retrapping case [12] whereas $b = 2$ is valid in the fast retrapping limit [13]. Nevertheless, in many cases close fit to experimental data are obtained with values between 1 and 2 [14], or even higher ones in some cases [15].

We have studied in previous works [16,17] the effect of the crystallization degree in the electrical relaxation obtained by TSDC in conventionally polarized (PET and PEN) electrets. The evolution of dipolar relaxations with the crystallinity degree showed a decrease in the intensity of the maximum associated with the decrease of the total amorphous fraction present in the sample [16]. The ρ relaxation showed a complex behavior with an initial increase, followed by a sharp decrease in the end of the crystallization process [17]. However, in conventional polarized samples the study of the ρ relaxation is difficult because all relaxations are activated simultaneously. In this paper, we make a deeper study of the space charge relaxations in PET and PEN as a function of the crystallinity degree in electrets formed by the WP method. In this case the relaxation kinetic parameters have been studied fitting the resulting depolarization current to the general order kinetics model.

2. Experimental

Commercial PEN (Kaladex 1030 from Cadillac Plastics and Chem. Co.) and PET (HostaPET from Hoechst Ibérica S.A.) sheets were used for the experiments. Amorphous samples were prepared quenching the molten sheet in water at room temperature. Samples with different crystallinity degrees were prepared by subsequent heating processes up to different final temperatures. The Thermal Stimulation by Steps method (TSS) [16,18] is represented schematically in Fig. 1. During the first heating process (a) the amorphous sample is heated to a temperature T_{f1} that produces some degree of crystallinity in the material. The partially crystallized sample is then cooled to temperatures below T_g (b) and heated again to $T_{f2} > T_{f1}$ (c), increasing further the crystallinity degree. This process is repeated to ever increasing final temperatures (T_{f3}, T_{f4},…) raising gradually the crystallinity degree of the material. One interesting advantage of this method is that when the sample is at a temperature around T_g it can be polarized by WP. In this process, the field is applied during the isothermal polarization time t_p. Then the sample is cooled to the initial temperature (T_0), and the TSDC discharge can be measured during the heating ramps. The heating rate used in all the ramps was 2.5°C/min.

Depolarization current measurements were carried out on 130 μm thick circular samples with 2 cm diameter aluminum electrodes on both sides of the sheet prepared by vacuum deposition. Short-circuit TSDC measurements were carried out on samples polarized by the WP method. The experimental set-up consisted of a measuring cell placed in an air-forced Kottermann-2715 oven, modified to be controlled by an Eurotherm model 818 temperature programmer. Temperature, during annealings and measurements, was measured to an accuracy of 0.1°C by Pt-100 probes located close to the sample. The discharge current was measured with a Keithley 610C electrometer. Data of temperature and current were collected by a PCLAB 814B A/D converter card in a personal computer. Calorimetric measurements (DSC) were performed with a Mettler TC11 thermoanalyser equipped with a DSC-20 Differential Scanning Calorimeter module. The calorimeter was previously calibrated with metallic standards (indium, lead, zinc). DSC curves were obtained from 10 mg samples. For DSC measurements the heating and cooling rates used

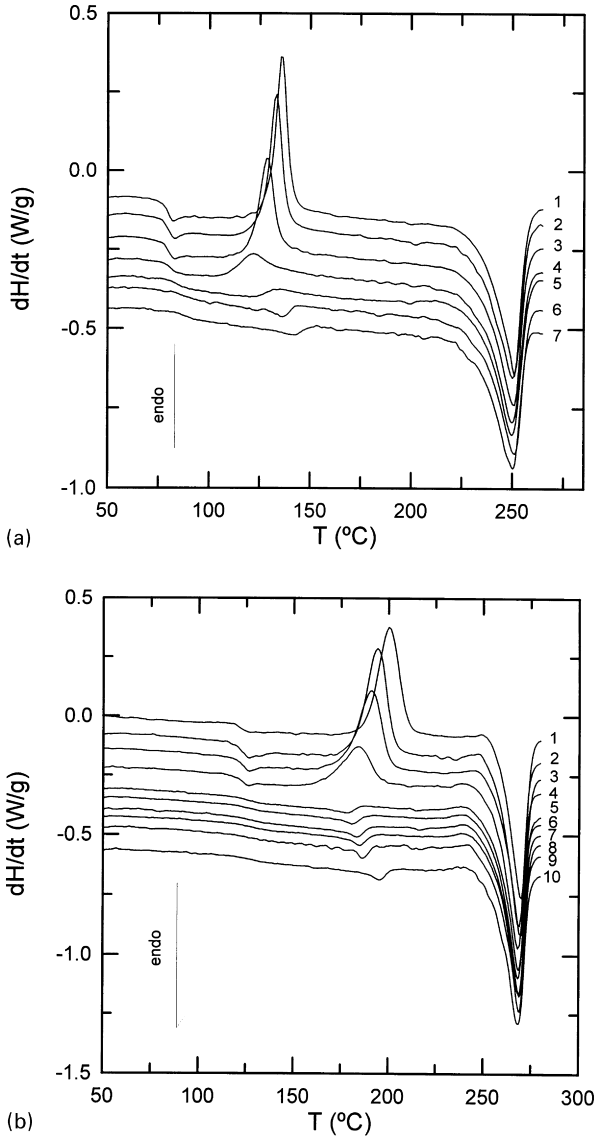

Fig. 2. DSC scans at 10°C/min. Samples were previously heated to different temperatures by the TSS method at 2.5°C/min. (a) PET T_f (°C): 105 (1), 110 (2), 112 (3), 114 (4) 128 (6) and 135 (7). (b) PEN T_f (°C): 158 (1). 160 (2), 163 (3), 166 (4), 172 (5), 175 (6), 177 (7), 178 (8), 180 (9) and 190 (10).

were, in all the ramps, 10°C/min and the measurements were carried out from 30 to 300°C. CuKα X-ray powder diffraction was recorded for 2θ angles between 8 and 60°.

3. Results and discussion

DSC measurements were carried out from 30 to 270°C, to characterize the glass transition, melting point and the crystallization behavior of the materials. Fig. 2 shows the results obtained for samples of PET (a) and PEN (b), treated by the TSS method up to different final temperatures. The glass transition of the materials is clearly observable in the scan corresponding to amorphous samples, and lies approximately at $T_g = 80$°C for PET and $T_g = 125$°C for PEN.

The crystallization process is a phase transformation where the polymer chains move toward lower energy configuration. For this reason, during this process important heat transfer between the sample and the environment take place. DSC technique was used to measure this heat transfer that is directly related to the progress of the crystallization process. The exothermic crystallization process of amorphous PET and PEN can be observed in curves 1–4 of Fig. 2a and b (T_f up to 114°C (PET) and 166°C (PEN)), at temperatures around 130 and 180°C, respectively. The melting process in both cases takes place at 270°C approximately. Curves 5–7 for PET (T_f from 118 to 135°C, Fig. 2a) and 5–10 for PEN (T_f from 172 to 190°C, Fig. 2b) do not show any crystallization process. This fact shows that these samples already have the highest degree of crystallinity achievable by TSS.

From the area of the exothermic and endothermic peaks, and the extrapolated heat of fusion for a pure crystal ($\Delta H_f = 126.7$ J/g (PET), $\Delta H_f = 103.3$ J/g (PET)), the crystallinity degree X_c of each sample can be estimated. Fig. 3a and b represent X_c as a function of the final temperature achieved in the TSS process (T_f). The evolution of X_c versus T_f can be fitted to an *tanh* function according to the following empirical equation:

$$X_c = A \tanh\lfloor B(T_f - C)\rfloor + D \quad (2)$$

where A, B, C and D are adjustable parameters that depend on the crystallization process. The B parameter shows an important decrease when the heating rate is increased, while the other parameters do not vary noticeably [19]. From Eq. (2) we can see that $D + A$ is equal to the maximum crystallinity degree achievable in the material and $D - A$ is equal to the initial crystallinity degree. When the sample is crystallized by the TSS method at 2.5°C/min. heating rate, the best fit is obtained for $A = 0.187$, $B = 0.268$ K^{-1}, $C = 112.5$ K and $D = 0.268$ (PET) and $A = 0.21$, $B = 0.328$ K^{-1}, $C = 165.8$ K and $D = 0.272$ (PEN). The calculated curves are represented in the figures as solid lines. This functional dependence allowed us to interpolate X_c for all the samples studied in this work.

It can be noted in Fig. 2 the appearance of a small endothermic peak in fully crystallized samples (curves 5–7 for PET and 5–10 for PEN). This endothermic peak increases in area and it shifts towards higher temperatures as T_f is increased, indicating that premelting processes occur in the material during these heat treatments. This behavior is related to important changes in the ρ relaxation (associated to free charge in the material) as Fig. 4 shows. This figure shows the TSDC curves obtained with PET (a) polarized by the WP method at $T_p = 86$°C for 20 min, and with PEN (b) polarized at $T_p = 130$°C for the same time ($V_p = 1.5$ kV in both cases).

We can see in these figures an initial increase in the ρ relaxation as the final temperature of the TSS process is increased, up to 118°C for PET (Fig. 4a) and 169°C for PEN (Fig. 4b). This initial increase is associated with the

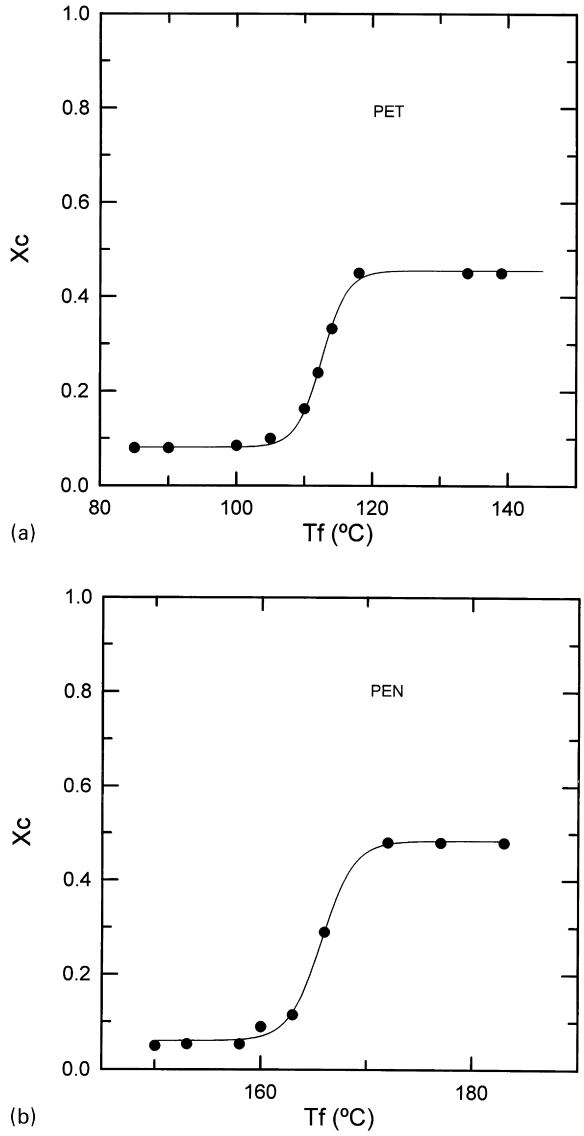

Fig. 3. Evolution of X_c versus T_f for samples treated by the TSS method up to different temperatures: (a) PET; and (b) PEN.

crystallization process of the material, as the DSC results represented in Fig. 2 show (curves 1–4). The maximum of the ρ peak corresponds, according to DSC results, to a fully crystallized sample, once the end of the crystallization process is reached.

When T_f is further increased the sample stays fully crystallized, however the ρ relaxation decreases drastically in both cases. This behavior occurs at the time the small endothermic peak appears in DSC measurements (Fig. 2), and simultaneously this peak shifts to higher temperatures.

The decrease in the ρ peak can be associated with the improvement of amorphous–crystal interfaces that occurs during the heat treatment at high temperature via the prefusion of irregular crystal interfaces or very small crystal like aggregates. This fact will produce the endothermic peak observed during the next DSC scan, and will reduce the number of interfacial charge traps present in the material with the consequent decrease in the ρ peak. To check this hypothesis a complete modelization of the ρ relaxation process as well as X-ray diffraction measurements of these samples have been carried out and are discussed below.

Fig. 4a and b show as well a slight shift of the peak maxima towards higher temperatures. This shift can be attributed to an increase in the depth of the traps. In the case of PET (Fig. 4a) a new peak emerges at temperatures close to 100°C, which predominates when the ρ peak is almost exhausted ($T_f = 123$°C sample). Previous works [20] showed that this peak (α_c) is associated with the glass transition of amorphous regions between the lamellae, inside the spherulites of the crystalline polymer.

3.1. Data modeling

Collected data were fitted to the general order kinetic equation. The integration of Eq. (1) for a constant heating rate (v) leads to

$$I = n_0 s_0 \exp\left(-\frac{E_a}{kT}\right) \times\left[\frac{(b-1)s_0}{v}\int_{T_0}^{T}\exp\left(-\frac{E_a}{kT}\right)dT + 1\right]^{-b/(b-1)} \quad (3)$$

This equation was employed to fit our experimental data. The fitting processes were performed by multidimensional minimization of the relative errors (maximum likelihood), with n_0, s_0, E_a and b as variable parameters. The routines on which our software is based are described by other authors [21]. We present in Fig. 5 a comparison between calculated and experimental data, to show the fitting accuracy of the model.

In Fig. 6, the evolution of the initial trapped charge (n_0) versus of the crystallinity degree (X_c) is displayed. In the region where X_c changes noticeably, the value of n_0 shows only a slight tendency to increase. A significant change in n_0 takes place once the sample has achieved maximum crystallinity degree detectable by DSC. In the case of PET, the α_c peak (related to the amorphous interlamelar regions) appears when the crystallinity degree attains values near the maximum. The appearance of the α_c peak makes unreliable the last two fittings. Even if it is not clearly visible, its influence introduces deviations of the experimental data from the general kinetic order model. The α_c peak is not so notorious in PEN and, therefore, the model can be used even when the sample has reached the maximum X_c. It is just at this point when n_0 begins to decrease. This behavior is due to changes in the microstructure, produced by the TSS method, which are not detectable by DSC. In the following, we will present further evidence to support this point of view.

The results about the preexponential factor and the activation energy are summarized in Table 1. The preexponential frequency factor (s_0) values found are orders of

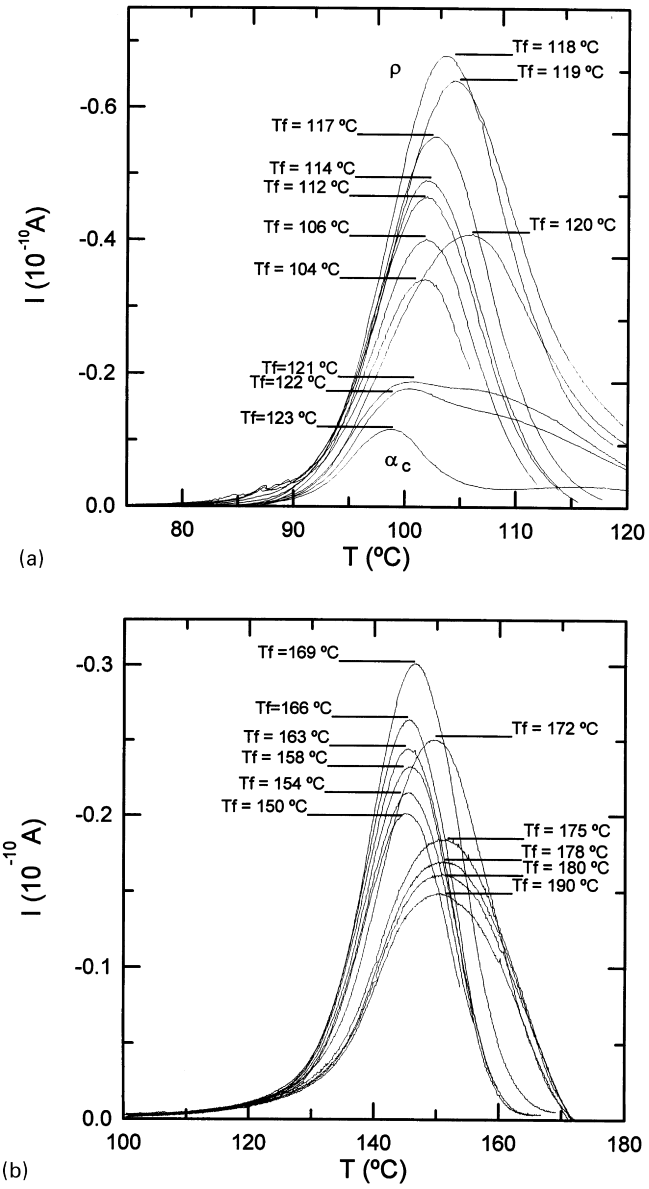

Fig. 4. Evolution of the ρ relaxation with the crystallinity degree obtained by TSDC of window polarized samples. (a) PET, $T_p = 86°C$, $T_o = 60°C$. (b) PEN $T_p = 130°C$, $T_o = 100°C$ ($V_p = 1.5$ kV and $t_p = 20$ min in both cases. T_f is indicated in the figure).

magnitude away from the Debye frequency (10^{13}–10^{14} Hz). In the case of the α relaxation such discrepancy is justified as the result of the cooperative character of molecular motions associated with the glass transition [22]. One can conclude that also for space charge relaxations, molecular motions are responsible for the high value of s_0 [7–9].

Another fact confirms the importance of molecular motion on space charge relaxation. As seen in Fig. 7, the plot of log (s_0) in terms of the activation energy (E_a) fits a compensation law [23,24]. It should be emphasized that s_0 and E_a are fully independent parameters in the general kinetic order model [7–9]. In spite of this fact, we have found a two-parameter relationship between these two magnitudes, which does not depend on the degree of crystallinity.

In Fig. 8, the kinetic order (b) is plotted against X_c. Like in the case of n_0, b is nearly constant as X_c grows and suffers a strong change when X_c attains the maximum value possible by TSS. For both polymers, it varies from a nearly constant value placed between $b = 1$ and $b = 2$ to a value close to $b = 3$.

Again, this behavior is interpreted as a consequence of changes in the microstructure that occur once X_c has reached its maximum value. These changes do not affect the crystallinity degree but they produce a radical change in the retrapping regime and, as we have discussed before, a noticeable variation in the initial number of trapped charge carriers.

Although these changes are not detected by DSC, other techniques can supply information about them. Fig. 9 shows the X-ray diffraction patterns of PET samples treated by the

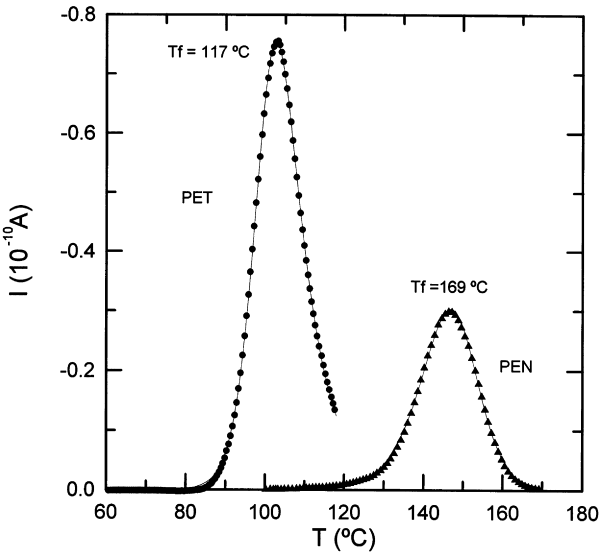

Fig. 5. Comparison between experimental and calculated TSDC data of the ρ peak. Two sets of experimental points are represented, one of PET (●) and another of PEN (▲). Calculated data is represented in both cases by a continuous line.

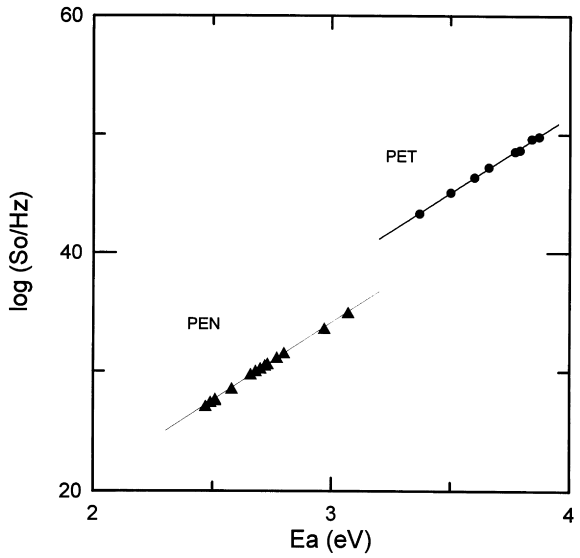

Fig. 7. Log s_0 versus E_a calculated for the ρ relaxation with different crystallinity degree PET (●) and PEN (▲). The linear dependence shows the validity of the Compensation law for this relaxation.

TSS method. Curves 1–3, which correspond to partially crystallized samples, show the appearance of diffraction peaks and their growth as the treatment proceeds. However, it is more interesting the evolution reproduced in curves 4–6, which correspond all of them to samples with the highest X_c (measured by DSC). In these curves, we can observe that the diffraction peaks show a refinement as the sample is treated further.

We can explain these results assuming that, when the sample is treated at high temperatures (but below the melting temperature) the pre-melting of irregular crystal interfaces or very small crystal-like aggregates occurs. This results in the improvement of the overall crystalline structure and, as a consequence, in the refinement of the observed diffraction peaks. Since charge traps are associated with amorphous–crystal interfaces, the improvement of the crystalline structure can explain both the decrease in the number of initial trapped charge and the modification of the retrapping regime.

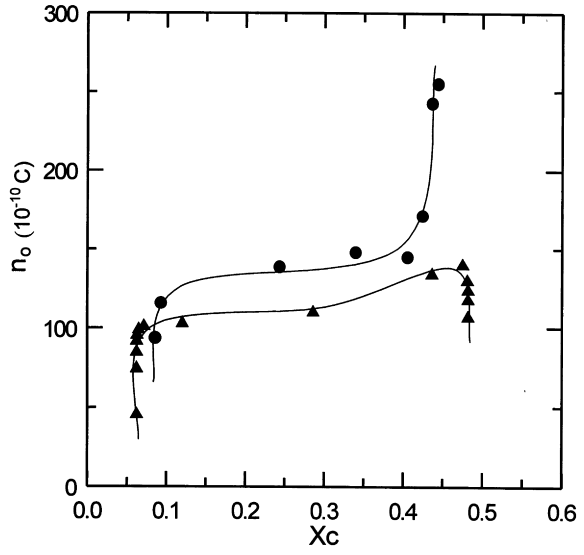

Fig. 6. Dependence of the initial trapped charge, n_0, with the crystallinity degree for PET (●) and PEN (▲) (Continuous lines are only indicative of the trend).

4. Conclusions

In this work we have successfully combined several techniques (DSC, TSDC and X-ray diffraction) to obtain a better knowledge about the influence of crystallization on free charge relaxation in PET and PEN. In addition, we address

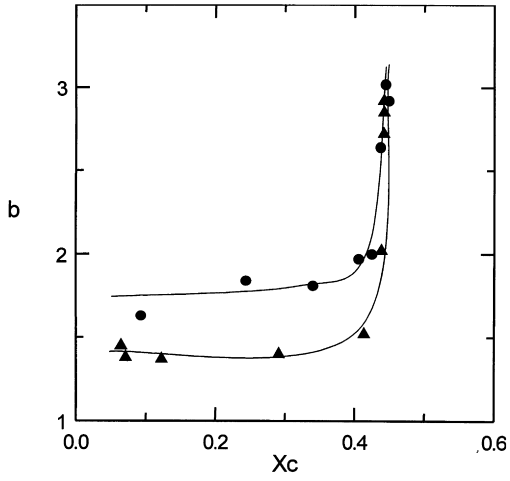

Fig. 8. Kinetic order parameter in front of the crystallinity degree for PET (●) and PEN (▲).

Table 1
Values of the preexponential factor (s_0) and the activation energy (E_a) for PEN and PET obtained during the mathematical fitting of the curves

PEN				PET			
T_f (°C)	X_c	s_0 (Hz)	E_a (ev)	T_f (°C)	X_c	s_0 (Hz)	E_a (ev)
145	0.062	9.3×10^{34}	3.0	104	0.08	2.2×10^{43}	3.3
150	0.062	4.1×10^{33}	2.9	106	0.09	1.3×10^{45}	3.5
154	0.062	3.6×10^{31}	2.8	112	0.24	1.7×10^{47}	3.6
156	0.062	1.4×10^{31}	2.7	114	0.33	2.5×10^{46}	3.6
158	0.064	4.6×10^{30}	2.7	116	0.40	4.3×10^{49}	3.8
160	0.070	6.1×10^{29}	2.6	117	0.42	3.7×10^{48}	3.7
163	0.122	1.1×10^{30}	2.6	118	0.43	6.6×10^{49}	3.8
166	0.290	3.2×10^{30}	2.7	119	0.44	4.9×10^{48}	3.7
169	0.413	1.8×10^{30}	2.7				
172	0.438	3.9×10^{28}	2.5				
175	0.441	1.3×10^{27}	2.4				
178	0.441	5.3×10^{27}	2.5				
180	0.441	4.2×10^{27}	2.5				

several issues about crystallization in these materials to explain the observed free charge behavior.

The use of WP has enabled us to employ a general kinetic order model that considers a unique relaxation time. The parameters of the model evolve within the crystallization process and reflect changes that occur in the microstructure of the material.

The crystallinity degree of the samples has been determined through DSC data. Anyway, some of the microstructural changes take place before the crystallinity degree (detected by DSC) of amorphous samples begins to increase or when it has already attained its maximum value.

In the last case, DSC scans show an endothermic peak while X-ray diffraction peaks become sharper. Therefore, we conclude that the prefusion of irregular crystal interfaces or small crystal aggregates produces an improvement of the amorphous–crystal interfaces. This explanation is compatible with the evolution of the parameters involved in the model. In the first case, a possible cause may be nucleation, although we have not found experimental evidence to support this idea.

Finally, the influence of molecular motion on free charge relaxation should be remarked about. This influence explains the existence of a compensation law, valid for samples with different crystallinity degrees, or the high value of the preexponential parameter.

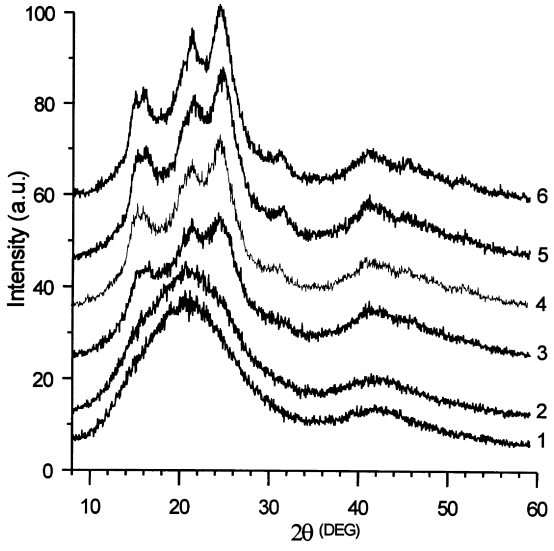

Fig. 9. X-Ray diffraction patterns of PET samples with different crystallinity degree. Previously, samples were heated up to 100°C (1), 110°C (2), 115°C (3), 140°C (4), 160°C (5) and 180°C (6) by the TSS method.

References

[1] Hinto T. J Appl Phys 1973;46:1956.
[2] Zielinski M, Kryszewski M. Phys Status Solidi 1977;46:305.
[3] Lacabanne C, Goyaud P, Boyer RF. J Polym Sci 1980;18:277.
[4] Gourari A, Bendaoud M, Lacabanne C, Boyer RF. J Polym Sci 1985;23:889.
[5] Montserrat P, Colomer P, Belana J. J Mater Chem 1992;2:217.
[6] Belana J, Mudarra M, Calaf J, Cañadas JC, Menéndez E. IEEE Trans Electrical Insulation 1993;28:287.
[7] Mudarra M, Belana J, Cañadas JC, Diego JA. Polym Sci B 1998;36:1971.
[8] Mudarra M, Belana J, Cañadas JC, Diego JA. Polymer 1999;40:2659.
[9] Mudarra M, Belana J. Polymer 1997;38:5815.
[10] Cañadas JC, Diego JA, Mudarra M, Belana J, Díaz-Calleja R, Sanchís MJ, Jaïmes C. Polymer 1999;40:1181.
[11] Belana J, Mudarra M, Cañadas JC, Calaf J, Menéndez E. IEEE Trans Electrical Insulation 1993;28:287.
[12] Randall JT, Wilkins MHF. Proc R Soc 1945;A184:366.
[13] Garlick GFJ, Gibson AF. Proc R Soc 1948;60:574.
[14] Swiatec J, Mandowski A. Trends in non-crystalline solids. In: Conde A, Conde F, Millán M, editors. Proceedings of the Third International Workshop on Non-Crystalline Solids, Matalascañas, November 1991, Singapore: World Scientific, 1992. p. 337.
[15] Chen R, Kirsh Y. Analysis of thermally stimulated processes, Oxford: Pergamon Press, 1981. p. 34.
[16] Belana J, Pujal M, Colomer P, Montserrat S. Polymer 1988;29:1738.
[17] Cañadas JC, Diego JA, Sellarès J, Mudarra M, Belana J, Díaz-Calleja, Sanchis MJ. Polymer 2000;41:2899.
[18] Colomer P, Montserrat S, Belana J. J Mater Sci 1998;33:1921.

[19] Cañadas JC. PhD thesis. Universitat Politècnica de Catalunya, Barcelona, 1999. p. 144.
[20] Diego JA, Cañadas JC, Mudarra M, Belana J. Polymer 1999;40:5355.
[21] Press WH, Flannery BP, Teukolsky SA, Vetterling WT. Numerical recipes. Cambridge: Cambridge University Press, 1986.
[22] del Val JJ, Alegria A, Colmenero J, Lacabanne C. J Appl Phys 1986;59(11):3829.
[23] Lacabanne C, Lamure A, Teussedre G, Bernes A, Mourgues M. J Non-Cryst Solids 1991;884:172–4.
[24] Moura Ramos JJ, Mano JF, Sauer BB. Polymer 1997;38(5):1081.